

# Renormalized Onsager functions and merging of vortex clusters

Franco Flandoli

Scuola Normale Superiore of Pisa

## Abstract

In this letter we numerically investigate the merging mechanism between two clusters of point vortices. We introduce a concept of renormalized Onsager function, an elaboration of the solutions of the mean field equation, and use it to understand the shape of the single cluster observed as a result of the merging process. We finally discuss the potential implications for the inverse cascade 2D turbulence.

*Introduction* - Stationary inverse cascade in 2D fluids with small scale activation and large scale friction is observed in experiments and quantified quite well by scaling laws, see the reviews [12], [2]. Dimensional analysis for the average square velocity increments  $u_r^2 := \langle |u(x+r) - u(x)|^2 \rangle$  assumes that  $u_r^2$  depends only on  $r$  and the energy flux  $\epsilon$  and has a scaling law  $u_r^2 = C\epsilon^\alpha r^\beta$ . Equating  $[L]^2/[T]^2$  to  $[L]^{2\alpha}/[T]^{3\alpha} \cdot [L]^\beta$  one immediately gets  $\alpha = \frac{2}{3}$  and  $\beta = \frac{2}{3}$ , namely  $u_r = C\epsilon^{1/3} r^{1/3}$ . This simple argument gives a result which was never contradicted by experiments. But it does not explain the mechanisms of the inverse cascade, it is based on assumptions which are not directly verifiable, and it gives the same result in 3D, where experiments reveal important deviations.

Vortex structures are certainly involved in the inverse cascade. One of the mechanisms which could be relevant is the aggregation of vortices in larger and larger clusters. This note aims to contribute to the understanding of one fragment of this complex process, namely the merging of two clusters of vortices into a larger one. Starting from the mean field equation of Onsager theory, we introduce the concept of renormalized Onsager function. It is a family of functions parametrized by a real number  $\beta$  (including the negative values promoted by Onsager) which correspond to unitary variance configurations and, properly rescaled, covers the class of all solutions of the mean field equation. We observe that the shapes emerging in very short time (between an half and one turnover time) from the merging of two roughly similar and close clusters of equal sign is very close to a renormalized Onsager function; more precisely, this is true in a class of numerical experiments, while in others there is a systematic deviation that requires further study but is addressed here by a first rough correction. Finally, we speculate how the results found here could be the starting point of a theory of inverse cascade, yielding also  $u_r = C\epsilon^{1/3} r^{1/3}$  (up to logarithmic corrections).

*Renormalized Onsager functions* - Consider  $N$  point vortices  $X_1, \dots, X_N$  in the plane, each one with circulation  $\Gamma$ ; the vorticity field is  $\frac{\Gamma}{N} \sum_{i=1}^N \delta(x - X_i)$ . Kinetic energy is infinite but modulated by the finite quantity (which corresponds to interaction energy)  $\mathcal{H} := -\sum_{i,j=1, i \neq j}^N \frac{\Gamma^2}{N^2} \log |X_i - X_j|$ , invariant for the vortex dy-

namics  $\frac{dX_i}{dt} = \sum_{j \neq i} \frac{\Gamma}{2\pi} \frac{(X_i - X_j)^\perp}{|X_i - X_j|^2}$ . Two other relevant invariants are the center of mass  $\mathcal{M} = \frac{1}{N} \sum_{i=1}^N X_i$  and the variance  $\mathcal{V} = \frac{1}{N} \sum_{i=1}^N |X_i - \mathcal{M}|^2$ , (related to the moment of inertia). Given two numbers  $e, \sigma$ ,  $\sigma \geq 0$  and a point  $m \in \mathbb{R}^2$ , consider the microcanonical measure formally defined by  $\mu_N^{e, \sigma, m} = \delta(\mathcal{H} = \Gamma^2 e, \mathcal{M} = m, \mathcal{V} = \sigma^2)$ . Onsager theory [10], [5], complemented by a more explicit formulation of the mean field equation by Montgomery and Joyce [9] and by various rigorous results (see for instance [3], [4], [6]) claims that

$$\int_{\mathbb{R}^{2N}} d\mu_N^{e, \sigma, m} \left| \frac{\Gamma}{N} \sum_{i=1}^N \varphi(x_i) - \Gamma \int_{\mathbb{R}^2} \varphi(x) \rho_{\alpha, \beta}(x - m) dx \right|^2$$

converges to zero for every smooth compact support test function  $\varphi$  on  $\mathbb{R}^2$ . Here the pair  $(\alpha, \beta)$  (with  $\alpha \geq 0$ ) is uniquely prescribed by  $(e, \sigma)$  and  $\rho_{\alpha, \beta}(x)$  is a probability density function given by  $\rho_{\alpha, \beta}(x) = Z_{\alpha, \beta}^{-1} e^{-\beta \phi_{\alpha, \beta}(x) - \alpha |x|^2}$ ,  $Z_{\alpha, \beta} = \int e^{-\beta \phi_{\alpha, \beta}(x) - \alpha |x|^2} dx$ , where  $\phi_{\alpha, \beta}(x)$  is the solution of the mean field equation

$$\Delta \phi_{\alpha, \beta}(x) = -Z_{\alpha, \beta}^{-1} e^{-\beta \phi_{\alpha, \beta}(x) - \alpha |x|^2}.$$

Uniqueness is true under the condition that the velocity  $\nabla^\perp \phi_{\alpha, \beta}$  vanishes at infinity and that  $\phi_{\alpha, \beta}$  is directly linked to the interaction energy  $\mathcal{H}$  above, which reduces to the condition  $\phi_{\alpha, \beta}(0) = -\frac{1}{2\pi} \int \log |x| \rho_{\alpha, \beta}(x) dx$ . A dynamical theory of convergence to equilibrium is however missing [5]. There are initial configurations, like those corresponding to rotation invariant profiles, having a time of convergence to equilibrium that is essentially infinite. However, other initial configurations have a much shorter relaxation time, if we accept some degree of approximation; this is what we want to describe with the following numerical experiments.

Solutions of the mean field equation are rotationally invariant; with little abuse of notation we shall write  $\rho_{\alpha, \beta}(r)$ ,  $\phi_{\alpha, \beta}(r)$  as functions of the distance to the center of mass. They have a special scaling property in  $\alpha$ : let us call *canonical* case the equation with  $\alpha = 1$ , whose solutions will be denoted by  $\rho_\beta(x)$ ,  $\phi_\beta(x)$ . In this case we impose  $\phi_\beta(0) = 0$  and  $\nabla \phi_\beta(0) = 0$ , convenient for numerical purposes (the condition  $\nabla \phi_\beta(0) = 0$  is motivated by radial symmetry and differentiability at the

origin). Then a simple computation shows that

$$\phi_{\alpha,\beta}(x) = \phi_\beta(\sqrt{\alpha}x) + C_{\alpha,\beta}, \quad \rho_{\alpha,\beta}(x) = \alpha\rho_\beta(\sqrt{\alpha}x)$$

$$Z_{\alpha,\beta} = \alpha^{-1}e^{-\beta C_{\alpha,\beta}}Z_\beta, \quad C_{\alpha,\beta} = \frac{1}{2\pi} \int \lg \frac{\sqrt{\alpha}}{|x|} \rho_\beta(x) dx.$$

Thus it is sufficient to know the shapes  $\rho_\beta(x)$ ,  $\phi_\beta(x)$  and rescale them as above.

However, comparing  $\rho_\beta(x)$  for different values of  $\beta$  is not so useful. In examples, we are given an initial family of vortex points with a value of  $(e, \sigma, m)$ . We should find a pair  $(\alpha, \beta)$  such that

$$\int \rho_{\alpha,\beta}(x) \phi_{\alpha,\beta}(x) dx = e$$

$$\int |x|^2 \rho_{\alpha,\beta}(x) dx = \sigma^2$$

(one can see that, with the prescriptions above,  $\Gamma^2 \int \rho_{\alpha,\beta}(x-m) \phi_{\alpha,\beta}(x-m) dx$  is the continuum analog of  $\mathcal{H}$ , and obviously  $\int |x-m|^2 \rho_{\alpha,\beta}(x-m) dx$  is the continuum analog of  $\mathcal{V}$ ). Although theoretically these equations are on the same ground, at a practical level the second one,  $\int |x|^2 \rho_{\alpha,\beta}(x) dx = \sigma^2$ , imposes a quite strict and stable constraint, while the first one is relatively poor, because the typical values of  $E$  are very small and with imperceptible, logarithmic variations for moderate changes of the initial configuration. Said differently, the value of  $\sigma$  is very relevant in practice, while the value of  $e$  is less easy to use in numerical experiments. The second equation gives us  $\alpha = \sigma^{-2} \int |x|^2 \rho_\beta(x) dx$ . Let us set  $\sigma_\beta^2 := \int |x|^2 \rho_\beta(x) dx$ . Thus, given an initial configuration with a value of  $\sigma$ , we may parametrize Onsager shapes directly by  $(\sigma, \beta)$ :

$$\rho_{\alpha,\beta}(x) = \sigma^{-2} \tilde{\rho}_\beta(\sigma^{-1}x), \quad \tilde{\rho}_\beta(x) := \sigma_\beta^2 \rho_\beta(\sigma_\beta x).$$

Notice that  $\int |x|^2 \tilde{\rho}_\beta(x) dx = 1$ . We call  $\tilde{\rho}_\beta$  *renormalized Onsager functions*. Comparing  $\tilde{\rho}_\beta(x)$  is the starting step to understand possible emerging shapes. In Figure 1 we compare the cases  $\beta = -15, 0, 30$  by plotting  $f_R(r) = 2\pi r \rho_{\alpha,\beta}(r)$ , the probability density function of the distance from the center of mass, and  $F_R(r)$ , the corresponding cumulative distribution function (cdf), which will be used below in numerical experiments.

The value of  $\sigma$  determines the typical distance of points from the center. The parameter  $\beta$  modulates only a little bit the shape. For  $\beta = 0$  the density  $\tilde{\rho}_0(x) = \sigma^{-2} Z_0^{-1} e^{-|\sigma^{-1}x|^2}$  is Gaussian, the maximum entropy distribution among those with a given variance, here equal to one. For  $\beta < 0$  the unitary variance constraint is maintained by means of more points close to the center of mass and more points far from it. For  $\beta > 0$  points tend to stay closer to unitary distance from the center of mass with respect to the Gaussian. In bounded domains

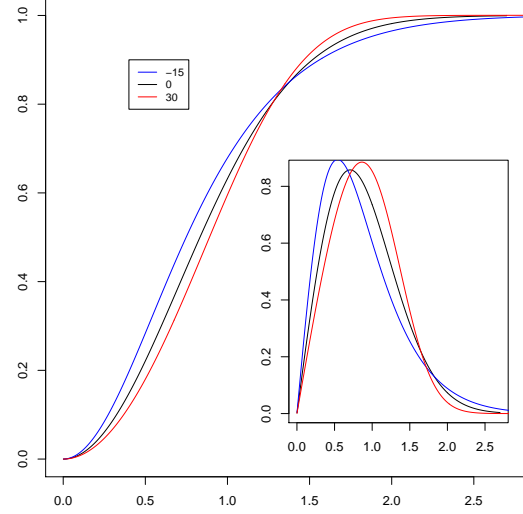


FIG. 1: Cdf of the distance from the center of mass for three examples of renormalized Onsager shapes,  $\beta = -15, 0, 30$  (pdf in the small figure).

the constraint of constant variance cannot be imposed and the role of  $\beta$  is more striking. Here in full space it plays a role of correction over the shape imposed by unitary variance.

Simulations of canonical Onsager mean field equation, for a given  $\beta$ , are made using the equation for the radial component

$$\frac{1}{r} \phi'_\beta(r) + \phi''_\beta(r) = -Z_\beta^{-1} e^{-\beta \phi_\beta(r) - r^2}$$

with  $\phi_\beta(0) = \phi'_\beta(0) = 0$ , finding the right value of  $Z_\beta = 2\pi \int_0^\infty e^{-\beta \phi_\beta(r) - r^2} r dr$  by iteration until the value is sufficiently stabilized. The nonphysical (but numerically useful) condition  $\phi_\beta(0) = 0$  is then removed by the constant  $C_{\alpha,\beta}$  above. The cumulative distribution function of the radius is computed as  $F_R(r) = -2\pi(\sqrt{\alpha}r) \phi'_\beta(\sqrt{\alpha}r)$ .

*Merging of two clusters* - In this section we investigate numerically the merging process between two clusters of point vortices, all with the same circulation, that we normalize so that the pair of clusters is globally a probability measure. The continuum limit, at time zero, is assumed to have the form

$$\omega_0(x) = \frac{1}{2} \rho_1 \left( x - \frac{d}{2} e_1 \right) + \frac{1}{2} \rho_2 \left( x + \frac{d}{2} e_1 \right)$$

$e_1 = (1, 0)$ , where  $\rho_1$  and  $\rho_2$  are probability densities, hence  $\omega_0$  is as well. The pdf  $\rho_1$  and  $\rho_2$  may be different and, up to small variations, will have unitary variance. By rescaling space and time, the understanding of this model case is representative of any size and any circulation. We approximate  $\omega_0(x)$  by two clusters of indepen-

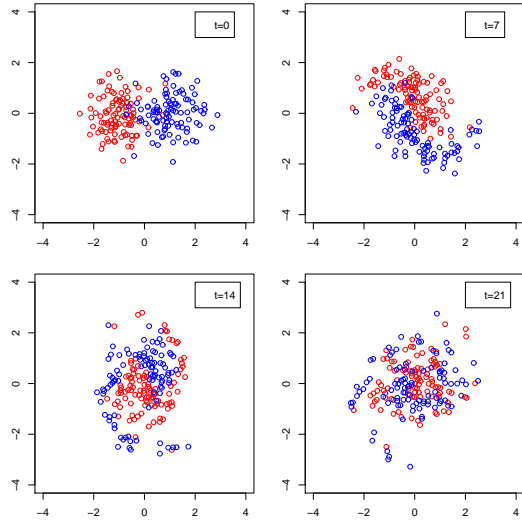


FIG. 2: Merging process of two unitary variance Gaussian clusters at distance  $d = 2$ . The four pictures show the initial configuration and three instances during the first turnover.

dent points

$$\frac{1}{2N} \sum_{i=1}^N \delta(x - X_i) + \frac{1}{2N} \sum_{j=1}^N \delta(x - Y_j)$$

with  $X_i$  (resp.  $Y_j$ ) distributed as  $\rho_1(x - \frac{d}{2}e_1)$  (resp.  $\rho_2(x + \frac{d}{2}e_1)$ ). When the distance  $d$  is large compared to the size  $r$ , the two structures rotate around their center of mass (and each one around its own center of mass) like two point vortices, just experiencing some degree of deformation of the circular structure in a roughly ellipsoidal one; this vortex-patch dynamics, approximating point vortex one, has been well understood by [8].

On the contrary, when  $d$  is small, typically of the order of 2 – 3 times the "radius" of the structures, the two clusters start immediately a merging process which evolves into a new larger cluster. Based on rigorous convergence results of point vortices to Euler equations [7], [11], we know that

$$\frac{1}{2N} \sum_{k=1}^{2N} \delta(x - Z_k(t)) \sim \rho(t, x) \quad (1)$$

namely  $Z_k(t)$  are distributed as the probability density  $\rho(t, x)$  which solves Euler equations with initial condition  $\omega_0(x)$ . The aim of our investigation is to identify an approximate shape for  $\rho(t, x)$ , based on Onsager theory, valid for relatively small  $t$  (around one turnover time). The initial configuration  $(X_i, Y_j, i, j = 1, \dots, N)$  lives on the surface  $\mathcal{H} = e$ ,  $\mathcal{V} = \sigma^2$ , but it is "anomalous" with respect to the typical configurations described by  $\rho_{\alpha, \beta}(x)$  with  $(\alpha, \beta)$  corresponding to  $(e, \sigma)$ . Statistical mechanics predicts convergence to  $\rho_{\alpha, \beta}(x)$ . As remarked above, in

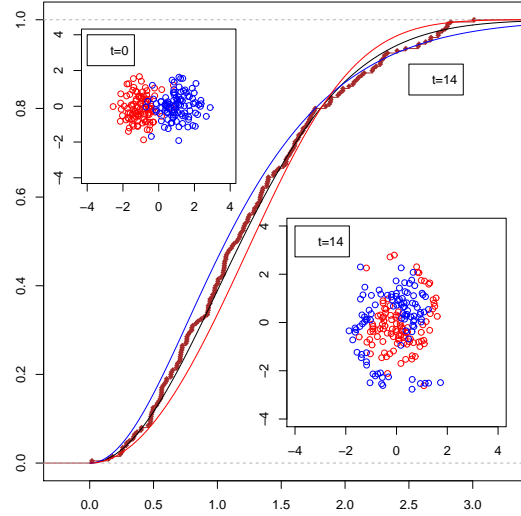


FIG. 3: Comparison between empirical cdf (of the distance from the center of mass) and Onsager renormalized functions for  $\beta = -15, 0.30$ , for the data of Figure 2.

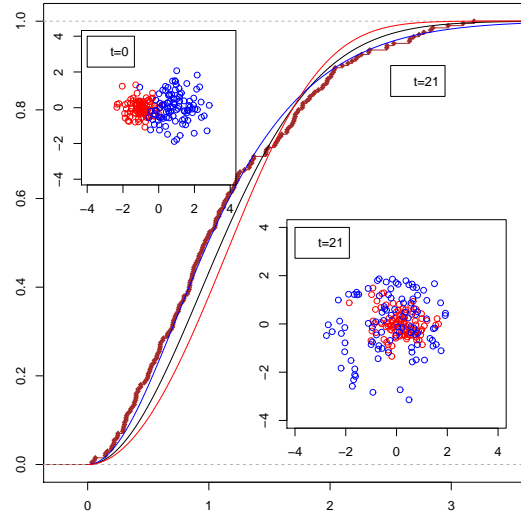


FIG. 4: An example with moderately different size of the initial clusters.

principle there are initial configurations which take too much time for convergence; what we observe numerically is a substantial approach to  $\rho_{\alpha, \beta}(x)$  in the time of one turnover or less.

We report several experiments. The first one is the case of two Gaussian clusters of unitary variance at distance  $d = 2$ . Turnover time is of the order of 20 sec (if space is measured in meters). The empirical cdf (ecdf), already between one-half and one turnover time, is very close to the class of Onsager functions, precisely to the Gaussian shape itself,  $\beta = 0$ . In Figure 2 we show vortex configurations at subsequent instants in the first turnover period of time, proving convergence towards a shape sub-

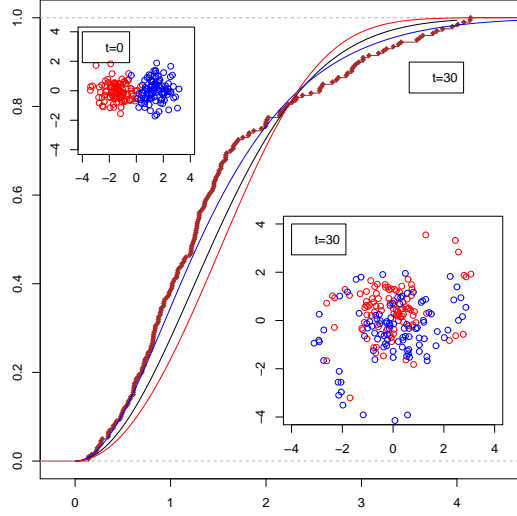


FIG. 5: Two unitary Gaussian clusters at distance  $d = 3$ . Deviation from renormalized Onsager functions is systematic.

stantially invariant by rotations. In Figure 3 we show the ecdf even before the first turnover time (later on it is substantially the same) superimposed to Onsager functions; we introduce the display, used also below, of the ecdf and, in small boxes the configurations at initial and final time.

This picture is partially stable under certain perturbations. In Figure 4 we show the case of two unequal initial Gaussian clusters. Here we clearly observe the choice, by the system, of negative  $\beta$ . In general negative  $\beta$  arise when, in the initial configuration, there is a remarkable quantity of vortex points more distant from the center of mass than the bulk of points. Under such conditions the system has a tendency to develop wings, namely to loose the boudary points through filamentary structures; while the bulk concentrates more, to compensate the distant points (due to conservation of variance). As remarked above when we discussed how renormalized Onsager functions change with  $\beta$ , this behavior corresponds to negative  $\beta$ .

*Deviation from renormalized Onsager functions* - When the dispersion of the initial configuration, in the sense just described above, is too large, the ecdf is vaguely similar to Onsager functions with  $\beta < 0$  but it shows also a systematic deviation. We illustrate this fact in Figure 5 with the case of two equal unitary Gaussian clusters at distance  $d = 3$  (instead of  $d = 2$ ). The phenomenology is similar to the one described above: wings of dispersed points and a strong kernel to compensate for the constant variance. But the shape is not Onsager anymore. We have not discover yet a variation of Onsager theory which may incorporate this case. However, a simple argument restores some fact. If we eliminate the extreme parts of the wings we observe again a good level of coincidence with renormalized Onsager functions. We show

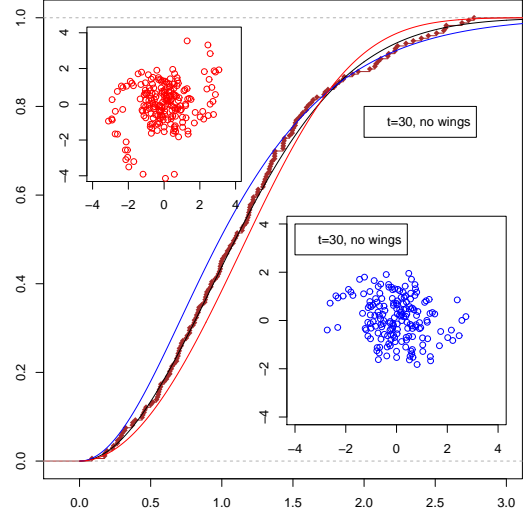


FIG. 6: Elimination of wings in the example of Figure 5. The original shape at time  $t = 30$  is in the upper box. The lower box and the ecdf correspond to the case without wings.

in Figure 6 the result after the elimination of the tails, in the case of the data of Figure 5.

*Potential relevance for inverse cascade* - Aggregation of vortex structures from smaller to larger ones is a well known phenomenon, clearly related to a cascade of energy from smaller to larger scales. What we may speculate after the observations of the previous sections is that a turbulent fluid may be composed, up to a disordered low-intensity component (which presumably includes the extremal parts of the wings formed during stretching processes), of localized intense vortex structures having approximatively a shape invariant by rotation and with radial distribution approximatively equal to a renormalized Onsager shape, rescaled by the standard deviation of the structure. These kind of structures are self-consistent, in the sense that two smaller ones merge into a larger one. The parameter  $\beta$  may vary and sometimes the Onsager shape can be attributed only to the bulk of the structure, dispersing the wings into the disordered background.

Assume the fluid is maintained in a stationary regime by injection of vortex structures at very small scale and dissipation by friction. Around every scale  $r_0$  we may assume to observe structures approximatively of that size, namely of the form  $r_0^{-2} \tilde{\rho}_{\beta_0} (r_0^{-1} x)$  where  $\tilde{\rho}_{\beta_0}$  is a renormalized Onsager function. When two such structures (with the same sign of circulation) are sufficiently close, they will merge into a new structure of the form  $r_1^{-2} \tilde{\rho}_{\beta_1} (r_1^{-1} x)$  with  $r_1 > r_0$  and some  $\beta_1$  (possibly up to elimination of extreme parts of wings). Admitting the unjustified simplicity of the next argument, let us assume we have an injection scale  $r_{injection}$  and, instead of a continuum of scales, only discrete scales

$$r_{injection} = r_{l_{inj}} < \dots < r_{l+1} < r_l < \dots < r_0$$

and that only merging events occur between structures of the same scale  $r_{l+1}$  (for some  $l$ ) producing structures of scale  $r_l$ ; and finally that there is a characteristic circulation  $\Gamma_l$  associated to scale  $l$ . The vorticity field has the form (up to a low-intensity disordered background)

$$\omega(x) = \sum_l \Gamma_l \sum_{i \in \Lambda_l} r_l^{-2} \tilde{\rho}_{\beta_i} (r_l^{-1} (x - x_i^0)) \quad (2)$$

where  $\Lambda_l$  indexes the set of structures of level  $l$ . Typical velocity at scale  $l$  is  $u_l = \frac{\Gamma_l}{r_l}$  (from Biot-Savart relation  $u(x) = \frac{1}{2\pi} \int \frac{(x-y)^\perp}{|x-y|^2} \omega(y) dy$ ). If we discover a relation between  $\Gamma_l$  and  $r_l$ , we find a formula for  $u_l$  as a function of  $r_l$ , to compare with the scaling law  $u_r = C\epsilon^{1/3} r^{1/3}$ .

Here  $\epsilon$  is the energy per unit of space-time injected at scale  $r_{l_{inj}}$  through the creation of the smaller vortex blobs. The system behaves like a stationary linear queuing network, with the same energy flux at each level  $l$ , and the rule  $\epsilon = \lambda_l \cdot \epsilon_l$ , where  $\epsilon_l$  is the kinetic energy of one structure of level  $l$ , while  $\lambda_l$  is the average number of "events" at level  $l$  in unit of space-time (either we choose to consider events the new arrivals, or we choose the departures, it is equivalent). Using the formula  $\int \int \log|x-y| \Gamma_l \rho_l(x) \Gamma_l \rho_l(y) dx dy$ , where we have abbreviated  $\rho_l(x) = r_l^{-2} \tilde{\rho}_{\beta_i} (r_l^{-1} (x - x_i^0))$ , we find  $\epsilon_l \sim \Gamma_l^2 \log \frac{1}{r_l}$ . Hence  $\epsilon \sim \lambda_l \cdot \Gamma_l^2 \log \frac{1}{r_l}$ . In queuing theory  $\lambda_l$  is the throughput, or average arrival/departure rate. A version of Little's law states that  $\lambda_l = \frac{n_l}{\tau_l}$  where  $n_l$  is the average number of structures involved in potential merging events and  $\tau_l$  is the merging time. By equilibrium considerations ( $n_l r_l^2 \sim$  area occupied by merging structures) it is reasonable to assume that  $n_l \sim \frac{C}{r_l^2}$  (this detail is more intricate than others and requires deeper investigation). The merging time at scale  $l$  for structures with circulation  $\Gamma_l$  is of the order  $\tau_l \sim \frac{r_l^2}{\Gamma_l}$ , by a simple computation based on the rescaling  $\omega(t, x) := \frac{r_l^2}{\Gamma_l} \omega_{r_l} \left( \frac{r_l^2}{\Gamma_l} t, r_l x \right)$ ; but essential is to assume that the merging time at unitary scale is unitary (up to a constant), fact that we observed in the numerical simulations above.

Collecting these facts we have  $\epsilon = \frac{n_l}{\tau_l} \epsilon_l \sim C \frac{\Gamma_l^3}{r_l^4} \log \frac{1}{r_l}$ . It follows

$$\Gamma_l \sim C \epsilon^{1/3} r_l^{4/3} / \log^{1/3} \frac{1}{r_l}$$

hence  $u_l \sim C \epsilon^{1/3} r_l^{1/3}$  (up to logarithmic corrections in  $r_l$ ) which gives the correct scaling law (logarithmic cor-

rections have been invoked in the literature [2], but experiments do not clarify this issue, due to few scales).

Turbulence is a non-equilibrium time-stationary system. The previous picture restores a very weak form of local equilibrium. In the classical form of local equilibrium, arbitrarily small macroscopic portions of the medium go to equilibrium in arbitrary short time. Here, convergence to equilibrium holds only for small but well defined portions of fluid and requires a *macroscopic time*, which does not go to zero with the size (it is an obvious consequence of the fact that particles, the point vortices, move at speed comparable to the macroscopic time). However this time is short,  $\tau_l \sim \frac{r_l^2}{\Gamma_l} \sim \epsilon^{-1/3} r_l^{2/3} \log^{1/3} \frac{1}{r_l}$  as discussed above, for vorticity configurations made of two close small vortex blobs.

As a final remark, from this picture emerges an approximate self-similar picture of the form (2) with suitable scaling laws of the parameters. We do not claim here that there is full self-similarity, this issue requires closer investigation, but it is not unreasonable. This structure, in the limit  $l_{inj} \rightarrow \infty$ , could be useful to investigate more advanced properties like the SLE structure of level lines [1]; the Poissonian structure emerging from the present description, by analogy with critical percolation, seems to be in favour of the conjecture SLE(6).

- 
- [1] D. Bernard, G. Boffetta, A. Celani, G. Falkovich, Nat. Phys. **2** (2006).
  - [2] G. Boffetta, R. E. Ecke, Annu. Rev. Fluid Mech. **44** (2012).
  - [3] E. Caglioti, P.L. Lions, C. Marchioro, M. Pulvirenti, Commun. Math. Phys. **174** (1995).
  - [4] G.L. Eyink, H. Spohn, J. Stat. Phys. **70** (1993).
  - [5] G.L. Eyink, K. R. Sreenivasan, Rev. Mod. Phys. **78** (2006).
  - [6] P.L. Lions, On Euler Equations and Statistical Physics, SNS, Pisa 1997.
  - [7] C. Marchioro, M. Pulvirenti, Mathematical Theory of Incompressible Nonviscous Fluids, Springer, New York 1994.
  - [8] C. Marchioro, M. Pulvirenti, Comm. Math. Phys. **154** (1993).
  - [9] D. Montgomery, G. Joyce, Phys. Fluids **17** (1974)
  - [10] L. Onsager, Suppl. Nuovo Cimento **279** (1949).
  - [11] S. Schochet, Comm. Pure Appl. Math. **91** (1996).
  - [12] P. Tabeling, Phys. Rep. **362** (2002).